HHS Public Access

Author manuscript

Nat Neurosci. Author manuscript; available in PMC 2015 September 01.

Published in final edited form as:

Nat Neurosci. 2015 March ; 18(3): 415–422. doi:10.1038/nn.3932.

Epigenetic basis of opiate suppression of *Bdnf* gene expression in the ventral tegmental area

Ja Wook Koo[1], **Michelle S. Mazei-Robison**[1,2], **Quincey LaPlant**[1], **Gabor Egervari**[1,3], **Kevin M. Braunscheidel**[4], **Danielle N. Adank**[4], **Deveroux Ferguson**[1], **Jian Feng**[1], **Haosheng Sun**[1], **Kimberly N. Scobie**[1], **Diane M. Damez-Werno**[1], **Efrain Ribeiro**[1], **Catherine Jensen Peña**[1], **Deena Walker**[1], **Rosemary C. Bagot**[1], **Michael E. Cahill**[1], **Sarah Ann R. Anderson**[1,3], **Benoit Labonté**[1], **Georgia E. Hodes**[1], **Heidi Browne**[1], **Benjamin Chadwick**[1,3], **Alfred J. Robison**[1,2], **Vincent F. Vialou**[1,5], **Caroline Dias**[1], **Zachary Lorsch**[1], **Ezekiell Mouzon**[1], **Mary Kay Lobo**[6], **David M. Dietz**[4], **Scott J. Russo**[1], **Rachael L. Neve**[7], **Yasmin L. Hurd**[1,3], and **Eric J. Nestler**[1]

[1]Fishberg Department of Neuroscience and Friedman Brain Institute, Icahn School of Medicine at Mount Sinai, New York, New York 10029, USA

[2]Department of Physiology, Michigan State University, East Lansing, MI 48824, USA

[3]Departments of Psychiatry and of Pharmacology and Systems Therapeutics, Icahn School of Medicine at Mount Sinai, New York, New York 10029, USA

[4]Department of Pharmacology and Toxicology, The State University of New York at Buffalo, Buffalo, NY 14214, USA

[5]Institut National de la Santé et de la Recherche Médicale, U952, Centre National de la Recherche Scientifique, Unité Mixte de Recherche 7224, UPMC, Paris, 75005, France

[6]Department of Anatomy and Neurobiology, University of Maryland School of Medicine, Baltimore, MD 21201, USA

[7]Department of Brain and Cognitive Sciences, Massachusetts Institute of Technology, Cambridge, MA 02139, USA

Abstract

Brain-derived neurotrophic factor (BDNF) plays a crucial role in modulating neural and behavioral plasticity to drugs of abuse. Here, we demonstrate a persistent down-regulation of exon-specific *Bdnf* expression in the ventral tegmental area (VTA) in response to chronic opiate exposure, which is mediated by specific epigenetic modifications at the corresponding *Bdnf* gene

Corresponding author: Eric J. Nestler, Fishberg Department of Neuroscience, Icahn School of Medicine at Mount Sinai, One Gustave L. Levy Place, Box 1065, New York, NY 10029. eric.nestler@mssm.edu.

Author contributions: J.W.K., M.S.M.-R., S.J.R., Y.L.H. and E.J.N. designed research; J.W.K., M.S.M.-R., Q.L., G.E., S.A.R.A., D.F., J.F., H.S., K.N.S., D.M.D.-W., E.R., C.J.P., D.W., R.C.B., B.L., G.E.H., H.B., B.C., A.J.R., V.F.V., C.D., Z.L., E.M., M.K.L. and D.M.D. performed the experiments; J.W.K. and R.L.N. generated viral vectors; J.W.K. and Q.L. analyzed data; J.W.K. and E.J.N. wrote the paper.

Competing Financial Interests: The authors declare no competing financial interests.

Note: Supplementary information is available in the online version of the paper.

promoters. Exposure to chronic morphine increases stalling of RNA polymerase II at these *Bdnf* promoters in VTA and alters permissive and repressive histone modifications and occupancy of their regulatory proteins at the specific promoters. Furthermore, we show that morphine suppresses binding of phospho-CREB (cAMP response element binding protein) to *Bdnf* promoters in VTA, which results from enrichment of trimethylated H3K27 at the promoters, and that decreased NURR1 (nuclear receptor related-1) expression also contributes to *Bdnf* repression and associated behavioral plasticity to morphine. These studies reveal novel epigenetic mechanisms of morphine-induced molecular and behavioral neuroadaptations.

Introduction

Brain-derived neurotrophic factor (BDNF) promotes the neural and behavioral plasticity induced by cocaine or other stimulant drugs of abuse via actions on the mesolimbic dopamine system, which is composed of dopamine neurons in the ventral tegmental area (VTA) of the midbrain and their anterior projections to the nucleus accumbens (NAc) and other forebrain regions[1–3]. Previous studies have shown that BDNF-TrkB activity and its downstream signaling cascades are induced in NAc by cocaine exposure[4–6]. In addition, manipulations that enhance BDNF signaling in the VTA-NAc circuit increase rewarding and locomotor responses to cocaine, while suppressing BDNF signaling has the opposite effect[5,7–10].

In striking contrast, we showed recently that chronic morphine suppresses *Bdnf* gene expression in mouse VTA and that such blockade enhances rewarding and locomotor responses to morphine by augmenting dopamine neuron activity[11]. Chronic opiates also induce some unique biochemical and morphological alterations in VTA, such as down-regulation of intracellular neurotrophin signaling cascades and reduced soma size of VTA dopamine neurons, effects not seen with stimulants[12–15]. Interestingly, some of these changes are reversed by direct administration of BDNF into this brain region.

Despite this evidence for an inverse relationship between BDNF activity in VTA and morphine action, the transcriptional mechanisms underlying *Bdnf* suppression by morphine are largely unknown. Here, we carried out a uniquely comprehensive analysis of epigenetic regulation at the *Bdnf* gene and demonstrate a series of interacting chromatin mechanisms in mediating morphine's down-regulation of *Bdnf* transcription in rat VTA.. We report that unique binding patterns of RNA polymerase II (Pol II), permissive and repressive histone modifications, their histone modifying enzymes and related regulatory proteins, and key transcription factors at specific *Bdnf* promoters are associated with morphine-induced *Bdnf* suppression in this brain region and with enhanced behavioral responses to opiates.

Results

Down-regulation of *Bdnf* expression in VTA by opiates

We first examined postmortem VTA sections of human brain and observed that heroin addicts, compared with matched controls (Supplementary Table 1), displayed reduced mRNA levels of *Bdnf* exon IX, which represents the protein-coding region of *Bdnf* mRNA

that is common to all *Bdnf* transcripts[16] (Fig. 1a and Supplementary Fig. 1a). *Bdnf* exon IX mRNA levels were also decreased in VTA of rats that chronically self-administered heroin (Fig. 1b and Supplementary Fig. 1b).

To further characterize VTA *Bdnf* gene regulation in opiate action, we used an extensively validated morphine treatment regimen, involving repeated IP injections, which is more amenable to higher throughput analyses. Rats received daily morphine injections (5 mg/kg) for 14 days and were examined 14 days later[17]. Having confirmed the expected sensitizing behavioral effects of chronic morphine in these rats (Supplementary Fig. 1c), we found that *Bdnf* exon IX expression was suppressed in VTA of chronic morphine-treated rats compared to saline controls (Fig. 1c) [one way ANOVA ($F_{3,32} = 3.872$, $p = 0.0181$) with Fisher's *post hoc* test, $p < 0.05$]. In contrast, acute morphine (5 mg/kg, IP) 14 days after chronic (14 days) saline treatment had no effect on *Bdnf* exon IX expression in rat VTA (Fisher's *post hoc* test, $p = n.s.$). However, subchronic morphine exposure (15 mg/kg, IP)—during 3 day-training for conditioned place preference (CPP)—was sufficient to decrease *Bdnf* exon IX expression in mouse VTA (Fig. 1d and Supplementary Fig. 1d). These findings demonstrate that repeated opiate exposure is required for *Bdnf* mRNA suppression in VTA across species, including human addicts, and supports the relevance of this adaptation to opiate action.

Stalling of Pol II at *Bdnf* promoters in VTA by morphine

Having established opiate suppression of *Bdnf* exon IX expression in VTA, we investigated the underlying mechanisms involved. Initial quantitative PCR (qPCR) analysis showed that *Bdnf* transcripts containing exons III, V, VII, or VIII are expressed at very low levels in rat VTA and show no significant changes after chronic morphine (Supplementary Fig. 1e). Thus, we focused on *Bdnf* transcript containing exons I, II, IV, and VI in VTA and observed thatchronic morphine also reduced *Bdnf* transcript levels of exons II, IV, and VI compared to saline controls (Fig. 2a,b). There was no difference in *Bdnf* exon I mRNA expression. These data show that the chronic morphine-induced suppression of *Bdnf* exon IX is attributable to reductions in exons II-, IV-, and VI-containing transcripts. Furthermore, the results demonstrate that such suppression is long-lasting: it persists for at least two weeks after cessation of morphine exposure, features suggestive of an epigenetic mechanism.

To understand the effect of chronic morphine on *Bdnf* gene transcription at the epigenetic level, we performed quantitative chromatin immunoprecipitation (qChIP) with an antibody that recognizes both non-phosphorylated and phosphorylated forms of Pol II (total-Pol II) and with antibodies that specifically recognize Pol II phosphorylated at either Ser2 or Ser5 at its C terminal domain. Ser5 hyper-phosphorylation at gene promoters and Ser2 hypo-phosphorylation in coding regions are thought to be hallmarks of stalled Pol II—associated with suppressed genes[18]. Total-Pol II binding to *Bdnf* promoter region 2 (*Bdnf*-p2), which corresponds to exon II, was higher in VTA of chronic morphine-treated rats relative to saline controls, with no changes seen at the other promoters (Fig. 2c). Phospho-Ser5-Pol II binding to *Bdnf*-p2, -p4, and -p6 in morphine-treated rats was increased (Fig. 2d). In contrast, phospho-Ser2-Pol II binding in coding regions was decreased at *Bdnf*-exon II (eII), -eIV, and -eVI after chronic morphine (Fig. 2e). These findings suggest sustained suppression of *Bdnf*-p2, -p4, and -p6 via Pol II stalling in VTA in response to chronic morphine.

Histone modifications at *Bdnf* promoters in VTA by morphine

Next, we conducted qChIP for numerous histone modifications at the four *Bdnf* promoters: three histone markers of gene activation, acetylated H3 (acH3), acH4, and trimethylation of Lys4 of H3 (H3K4me3); three markers of gene repression, H3K9me2, H3K9me3, and H3K27me3; and one marker of transcription elongation, H3K36me3. Chronic morphine-exposed animals displayed clear patterns of histone regulation at *Bdnf* promoters in VTA (Supplementary Fig. 2a–g), with the most pronounced regulation occurring, as with Pol II, at *Bdnf*-p2. The changes observed in morphine-treated rats represent modifications induced by chronic morphine which persisted despite 2 weeks of abstinence: acH3 was decreased, while H3K4me3 and H3K27me3 were increased, at *Bdnf*-p2 compared to saline controls (Fig. 3a). No changes in acH3, H3K4me3, or H3K27me3 were seen at *Bdnf*-p1, -p4, and -p6 after morphine exposure (Supplementary Fig. 2a–g). In addition, we observed no significant alterations in H3K9me2, H3K9me3, or H3K36me3 at any *Bdnf* promoters, whereas elevated acH4 levels at *Bdnf*-p4 were observed in morphine-treated rats.

As follow up, we performed qChIP for key histone modifying enzymes and related regulatory proteins associated with a given histone mark, such as mSIN3a (mammalian SIN3 transcription regulator family member A), ING2 (inhibitor of growth 2), MLL1 (mixed-lineage, leukemia; KMT2A, lysine-specific methyltransferase 2A), G9a (EHMT2, euchromatic histone-lysine N-methyltransferase 2), and Polycomb group proteins. Since mSIN3a is a core component of a prominent co-repressor complex implicated in numerous systems[19], we examined the binding of this protein to *Bdnf* promoters. We found that mSIN3a binding to *Bdnf*-p1, -p2, and -p6 was robustly increased in VTA after chronic morphine (Fig. 3b and Supplementary Fig. 2h). We examined the binding of ING2 to *Bdnf* promoters, based on our paradoxical observation of increased H3K4me3 levels at *Bdnf*-p2 in VTA of morphine-treated rats. H3K4me3 typically denotes increased gene transcription, however, there is evidence that ING2 represses particular genes by binding to H3K4me3 and recruiting the mSIN3a repressive complex[20,21]. We found that ING2 binding to *Bdnf*-p1, -p2, -p4, and -p6 was dramatically increased in VTA in response to chronic morphine (Fig. 3b and Supplementary Fig. 2i). Such recruitment of ING2 and mSIN3a to *Bdnf* promoters explains why an increase in H3K4me3 is associated with gene repression. Consistent with our H3K4me3 data, morphine-treated rats showed elevated binding of an H3K4 methyltransferase, MLL1, to *Bdnf*-p2 and -p6 in VTA (Fig. 3c and Supplementary Fig. 2j). In contrast, an H3K9 methyltransferase, G9a, exhibited no changes in binding to *Bdnf* promoters, consistent with the lack of alterations in H3K9me2 levels (Fig. 3d and Supplementary Fig. 2k).

H3K27me3-mediated gene repression is associated with Polycomb group proteins, which reside in two main complexes: PRC1 (Polycomb repressive complex 1) and PCR2. PRC2 contains SUZ12 (zinc finger protein suppressor of zeste 12) and EZH2 (enhancer of zeste homologue 2); the latter catalyzes H3K27me3[22,23]. PRC1, which contains BMI1, RING1A, and RING1B, contributes to histone H2A monoubiquitination and interactions of Polycomb group proteins with H3K27me3[24,25]. Consistent with increased levels of H3K27me3 at *Bdnf*-p2, the binding of PRC2 complex proteins—namely, SUZ12 and EZH2—to *Bdnf*-p2 was increased in VTA by chronic morphine (Fig. 3e). High levels of occupancy by EZH2,

but not SUZ12, were also found at *Bdnf*-p4 and -p6 (Supplementary Fig. 2l,m). In contrast, binding of PRC1 complex proteins such as RING1A to *Bdnf*-p2 was reduced by morphine, whereas no changes were seen at other *Bdnf* promoters or in RING1B and BMI1 binding at any promoter (Fig. 3f and Supplementary Fig. 2n,o,p). Together, this comprehensive analysis of epigenetic regulation of the *Bdnf* gene in VTA by chronic morphine demonstrates concerted modifications predominantly at *Bdnf*-p2 that are consistent with transcriptional repression (Supplementary Fig. 2q).

To test directly whether alterations in H3K27me3 in VTA influence *Bdnf* expression and morphine-elicited behavioral changes, we generated a Herpes Simplex Virus (HSV) vector to overexpress EZH2 selectively in VTA compared to HSV-GFP controls (Fig. 3g and Supplementary Figs. 3a and 4a). Such EZH2 overexpression, which was selective for VTA and not seen in neighboring brain regions (Supplementary Fig. 4a), reduced *Bdnf* mRNA levels in VTA (Fig. 3h) and robustly increased morphine CPP (5 mg/kg) in mice (Fig. 3i). In contrast, intra-VTA infusion of a lentiviral vector expressing a short hairpin interfering RNA of *Ezh2* (i.e., LV-shRNA-EZH2), which repressed *Ezh2* mRNA expression (Supplementary Fig. 3b,c), blocked the morphine-induced reduction of *Bdnf* expression in VTA (Supplementary Fig. 3d).

Regulation of CREB binding to *Bdnf* promoters by morphine

We next examined CREB (cAMP response element-binding protein), which induces *Bdnf* in other systems[26]. Total-CREB binding to *Bdnf*-p6 was increased in VTA in chronic morphine-treated rats, with no changes seen at the other promoters (Fig. 4a). However, the binding of phospho-CREB (its active form) to *Bdnf*-p1, -p2, and -p4 was robustly decreased under these conditions (Fig. 4b). To confirm the direct connection between CREB activity and *Bdnf* expression in VTA, we infused HSV-CREB into VTA of wildtype mice to overexpress CREB selectively in this region (Fig. 4c). CREB overexpression augmented *Creb1* mRNA and protein levels selectively in VTA (Supplementary Figs. 4b and 5a); it also increased *Bdnf* mRNA expression in VTA compared to HSV-tdTomato (TMT) controls (Fig. 4d). Conversely, knocking down CREB by infusing HSV-Cre into the VTA of floxed CREB mice (Fig. 4e and Supplementary Fig. 5b) decreased *Bdnf* expression compared to HSV-GFP controls (Fig. 4f).

Next, we addressed how chronic morphine suppresses phospho-CREB binding selectively to *Bdnf* even though chronic morphine increases overall CREB activity in this brain region[27,28]. We tested the hypothesis that elevated H3K27me3 suppresses phospho-CREB binding to *Bdnf* promoter regions, since a recent study showed that H3K27me3 antagonizes CREB activity and represses expression at certain gene promoters in lymphocytes[29]. EZH2 overexpression by itself (i.e., without morphine), which increased H3K27me3 levels at all *Bdnf* promoters (Fig. 4g), decreased phospho-CREB binding to all *Bdnf* promoters (Fig. 4h). Moreover, in contrast to the morphine-induced decrease in phospho-CREB binding to the *Bdnf* promoters, phospho-CREB binding was increased by chronic morphine at the promoters of *Th* (tyrosine hydroxylase) and *Gria1* (GluA1 AMPA receptor subunit), two known CREB target genes that are induced in rodent VTA under these conditions[27,28] (Supplementary Fig. 6a,b). H3K27me3 levels at *Th* and *Gria1* were not affected in VTA by

chronic morphine (Supplementary Fig. 6c). In contrast to *Bdnf* repression by EZH2 overexpression, *Th* and *Gria1* expression was not altered by EZH2 in mouse VTA (Supplementary Fig. 3a). Heroin self-administration also decreased phospho-CREB binding to all *Bdnf* promoters (Supplementary Fig. 6d,e) and increased H3K27me3 at *Bdnf*-p1, -p2, and -p4 (Supplementary Fig. 6f).

Regulation of NURR1 binding to *Bdnf* promoters by morphine

We also examined the transcription factor NURR1 (nuclear receptor related 1), since it regulates several genes including *Bdnf* in midbrain dopamine neurons[30–33]. NURR1 binding to *Bdnf*-p1 and -p2 was decreased in VTA of chronic morphine-treated rats (Fig. 5a). Interestingly, chronic morphine suppressed *Nurr1* mRNA expression in VTA, an effect also seen in heroin self-administering rats (Fig. 5b,c), which could explain the reduced NURR1 binding to *Bdnf* promoters. Consistent with *Nurr1* suppression, H3K27me3 binding at the *Nurr1* promoter in VTA was increased by chronic morphine (Fig. 5d). Furthermore, we examined the relationship between CREB and NURR1 in response to chronic morphine, since *Nurr1* is a known downstream target of CREB in other systems[32,34]. Chronic morphine decreased phospho-CREB binding to the *Nurr1* promoter in VTA (Fig. 5e), while CREB overexpression in mouse VTA using HSV-CREB, which induced total- and phospho-CREB binding to the *Nurr1* promoter (Supplementary Fig. 5c,d), robustly augmented *Nurr1* mRNA expression in this region (Fig. 5f). The induced H3K27me3 and reduced phospho-CREB binding at *Nurr1* in VTA in response to chronic morphine suggest an antagonistic relationship between H3K27me3 and phospho-CREB, as observed for the *Bdnf* promoter under these conditions.

We generated and validated an HSV vector to overexpress NURR1 and examine its functional role selectively in VTA (Supplementary Figs. 4c and 7a). We first infused HSV-NURR1 into rat VTA 10 days after the last injection of our standard 14 day chronic morphine paradigm (5 mg/kg, IP). Rats were then re-exposed to morphine (5 mg/kg, IP) 4 days after the HSV-NURR1 infusion (Fig. 5g); such re-exposure (M/M) induces higher locomotor responses compared to a saline challenge (M/S) (see Supplementary Fig. 1c). We observed that NURR1 overexpression in VTA blocked this hyper-locomotion by morphine re-exposure (Fig. 5h and Supplementary Fig. 7b). We also investigated the influence of NURR1 on morphine reward using the CPP paradigm. We first confirmed that NURR1 overexpression induced *Bdnf* expression in mouse VTA, as observed in rat (Fig. 5i,j), and then demonstrated that morphine reward was also blocked by NURR1 overexpression in mouse VTA (Fig. 5k). Importantly, NURR1 overexpression in VTA of mice lacking BDNF in this brain region (generated by infusing HSV-Cre into VTA of floxed BDNF mice) did not show the suppressive effect of NURR1 overexpression on morphine reward (Fig. 5l), which provides a direct link between NURR1 action and regulation of BDNF activity in this brain region.

Discussion

Consistent with prior reports of opiate regulation of VTA BDNF expression[11,35] (but see[36]), the present study shows that *Bdnf* mRNA levels are robustly reduced in VTA of human

heroin addicts, of heroin self-administering rats, and of repeated morphine-treated mice (including those undergoing CPP). We observed that chronic morphine exposure induces a robust and sustained decrease in levels of specific *Bdnf* exon transcripts (i.e., *Bdnf* exons II, IV, and VI) in this brain region in rats. A uniquely comprehensive analysis of epigenetic mechanisms—particularly for a micronucleus such as VTA—revealed that this *Bdnf* suppression by chronic morphine is associated with a series of interacting and sustained transcriptional and chromatin modifications at the corresponding *Bdnf* gene promoters. In particular, we found that chronic morphine decreases binding of the active (phospho-Ser2) form of Pol II within *Bdnf*-eII, -eIV, and -eVI, whereas phospho-Ser5 Pol II binding to *Bdnf*-p2, -p4, and -p6 was augmented in VTA. These findings suggest that chronic morphine induces a sustained Pol II stalling at certain *Bdnf* promoters in concert with the gene's sustained repression.

Such stalling of Pol II is associated with several other key chromatin changes, with the most robust regulation seen at *Bdnf*-p2 in VTA (see Supplementary Fig. 2q). Consistent with repression of *Bdnf*-p2, we demonstrated increased binding of H3K27me3, a major form of repressive histone methylation. Occupancy by the PRC2 complex including SUZ12 and EZH2, which mediates H3K27 trimethylation[22,23], at *Bdnf*-p2 in VTA is also increased by chronic morphine. We provide a causal connection between H3K27me3 and **s**uppression of the *Bdnf* gene in VTA by showing that EZH2 overexpression in this region decreases *Bdnf* expression, while EZH2 knockdown blocks morphine's *Bdnf* suppression. Together, these data support a scheme whereby PRC2-mediated H3K27me3 reduces *Bdnf* gene expression (Supplementary Fig. 8). Interestingly, PRC2 has been shown to interact with other repressor proteins, in particular, with mSIN3a and related proteins[37,38], which are also enriched at *Bdnf*-p2 in VTA in response to chronic morphine. Consistent with our previous study, which linked reduced levels of VTA BDNF with increased morphine reward[11], we show here that EZH2 overexpression in VTA promotes this morphine-elicited behavior as well.

Repression of *Bdnf*-p2 is associated with increased levels of H3K4me3, which is typically related to gene activation. This observation illustrates the complexity of chromatin regulatory mechanisms *in vivo*. Insight into this complexity is provided by our observation that this paradoxical increase in H3K4me3 is associated with induction of ING2 binding to *Bdnf*-p2 by morphine. ING2, also a subunit of the repressive mSIN3a complex, binds with high specificity to H3K4me3 and consequently represses transcription of certain genes[20,21]. We show further that this unusual, but precedented, interaction between H3K4me3 and the mSIN3a/ING2 also involves the morphine-induced recruitment of the H3K4-specific methyltransferase, MLL1[39], to *Bdnf*-p2 (see Supplementary Fig. 8). Interestingly, MLL1, like its H3K4me3 mark, has been shown to interact with repressive complexes at particular genes in other systems[40].

The morphine-induced *Bdnf* repression also involves reduced binding of a key transcription factor, phospho-CREB, which has previously been shown to induce *Bdnf* gene expression in other systems[26]. However, the reduced phospho-CREB binding to *Bdnf* promoters in VTA after chronic morphine is surprising, since chronic morphine increases total levels of phospho-CREB and CREB transcriptional activity in VTA[27,28]. These findings suggest that there are specific features at *Bdnf* promoters responsible for the exclusion of phospho-CREB

after chronic morphine. We show that one mechanism for this exclusion is the induction of H3K27me3, since EZH2 overexpression—which induces H3K27me3—in VTA in the absence of morphine reduces phospho-CREB binding to *Bdnf* promoters. A recent study has reported that PRC2 occupancy and increased H3K27me3 at certain gene promoters antagonizes CREB binding to silence gene expression in lymphocytes[29]. In contrast, phospho-CREB binding to the promoters of *Th* and *Gria1*, two known targets of phospho-CREB in VTA[28], were increased in response to chronic morphine as would be expected. It is notable that chronic morphine did not affect H3K27me3 levels at *Th* and *Gria1* promoters and that *Th* and *Gria1* mRNA expression was not altered by EZH2 overexpression in contrast to *Bdnf* expression. While a caveat of these studies are potential off-target effects of overexpressed transcription factors, our findings together suggest that reduced phospho-CREB binding to *Bdnf* promoters is mediated by the selective recruitment of H3K27me3 to key *Bdnf* promoters during a course of opiate exposure.

Bdnf gene regulation is also known to be controlled by NURR1, which is required for maintenance of adult dopamine neurons in VTA[33]; NURR1 acts downstream of CREB[32,34] and upstream of BDNF[31,32]. This connection between CREB and NURR1 is supported by our data that *Nurr1* mRNA expression is induced in VTA upon CREB overexpression. This finding supports the hypothesis that the morphine-induced reduction in phospho-CREB binding to the *Nurr1* promoter demonstrated in this study mediates the *Nurr1* suppression in VTA by chronic morphine. In parallel, we found that *Nurr1* mRNA levels and NURR1 binding to *Bdnf* promoters are decreased in this region by morphine. Our observation that *Bdnf* mRNA levels are increased in VTA upon NURR1 overexpression is consistent with the scheme that reduced NURR1 binding to *Bdnf* promoters contributes to *Bdnf* suppression in response to morphine. This scheme is also supported by our behavioral data: chronic morphine-induced locomotor responses, as well as morphine-elicited reward, are blocked by NURR1 overexpression in VTA. Since NURR1 overexpression induces *Bdnf*, these behavioral data are consistent with prior reports that elevated VTA BDNF activity is also associated with suppression of morphine's behavioral effects[11]. Such a connection between NURR1 and BDNF was established by our demonstration that NURR1's ability to suppress morphine-elicited behaviors was lost in mice lacking BDNF selectively in this brain region.

In conclusion, our findings reinforce the complexity of gene and chromatin regulation in adult brain and emphasize the importance of examining numerous chromatin endpoints when investigating epigenetic mechanisms of gene regulation *in vivo* (Supplementary Fig. 8). Given that morphine suppression of *Bdnf* in VTA contributes importantly to the drug's behavioral effects[11], results of the present study provide fundamentally new insight into the detailed molecular mechanisms underlying morphine-induced neural and behavioral plasticity.

Online materials and methods

General Methods

Animals—Male 8–10 week-old Sprague Dawley rats (225–250 g; Charles River) were used in all experiments unless otherwise noted, given the larger size of their VTA, which makes detailed epigenetic studies possible. In some experiments, male 7–8 week-old

c57BL/6 mice (25–30 g, Jackson), and 9–13 week-old floxed CREB and floxed BDNF mice were used. Floxed CREB mice on a c57BL/6 background and floxed BDNF mice on a BL6/sv129 background were generated and maintained, as previously described[41,42]. These mice were used for key behavioral experiments in order to take advantage of genetic mutants. All animals were housed in groups of 2 rats or 2–5 mice per cage at 22–25°C on a 12-hr light/dark cycle (lights on 7:00 AM) with access to food and water *ad libitum*. Animals were acclimated to vivarium conditions for at least one week before experimentation and assigned randomly to experimental groups. All behavioral experiments, except self-administration, were performed during the light cycle. All animals used were experimentally naïve. All work was in accordance with guidelines of the Society for Neuroscience and the Mount Sinai IACUC.

Human postmortem subjects—Postmortem human brain specimens from heroin users and control subjects were collected within ~24 hr after death under approved protocols at the Department of Forensic Medicine at Semmelweis University, Hungary, or the National Institute of Forensic Medicine, Karolinska Institutet, Stockholm, Sweden. Brains were immediately frozen using dry-ice–cooled isopentane, cryosectioned, and thaw-mounted onto poly-l-lysine–treated slides. Cause and manner of death were determined by a forensic pathologist after evaluating the circumstances of death, toxicology data (blood, urine, and liver), and autopsy results. Information was also evaluated from police reports, family and friends, and medical records as described in Supplementary Table 1. Inclusion criteria were death associated with heroin intoxication (verified by toxicology), physical signs of heroin use such as needle tracks, and history of heroin abuse. Exclusion criteria were postmortem interval (PMI) of >24 hr, age <20 years, HIV-positive status, and history of alcoholism.

Heroin self-administration—Heroin self-administration in rats was conducted according to published procedures[43].

Morphine CPP—An unbiased CPP paradigm was used according to published procedures[11].

Locomotor activity—Rats were given morphine (morphine sulfate in saline, 5 mg/kg, IP) or saline daily for 14 days and then challenged with morphine (5 mg/kg, IP) or saline on day 28. On day 0, 14, and 28, morphine or saline was administered after 30 min habituation in the locomotor chamber. Locomotor activity was monitored for 30 min after the administration using the Photobeam Activity System (San Diego Instruments).

HSV vectors—HSV-GFP was generated with the p1005+ HSV amplicon bicistronic plasmid containing a complete CMV-GFP expression cassette as the second cistron. For HSV-NURR1, we designed the forward primer with *Kpn*I restriction sites (5′-GGGGTACCCCATGCCTTGTGTTCAGGCGCAGTATG-3′) and reverse primer with *Xho*I restriction sites (5′-CCGCTCGAGCGGTTAGAAAGGTAAGGTGTCCAGGAAA-3′). The PCR products for *Nurr1* were then digested, purified, and ligated into the first cistron downstream of the HSV IE4/5 promoter of the HSV amplicon at *KpnI-Xho*I. For HSV-EZH2, the coding sequences for *Ezh2* from pCMV-HA hEZH2 (Addgene plasmid #24230) were subcloned into the HSV amplicon at *EcoR*V-*BamH*I. Viral titers were determined

using qPCR and ~1×10^9 particles/site were used. All behavioral experiments were initiated ≥2 days and completed <5 days after viral injection, the time period when HSV expression is maximal. HSV-CREB and HSV-Cre vectors have been described previously[44,45]. Viral targeting to VTA was confirmed for all animals; <3% were excluded for anatomically incorrect placements. For validation of viral-mediated gene transfer, rat or mouse VTA bilateral punches (rat, 14-gauge; mouse, 15-gauge) were dissected under fluorescent stereomicroscope (Leica MZ10F) 4 days after intra-VTA infusion of the HSVs and processed for qPCR as described below (Supplementary Figs. 3a, 5a,b and 7a). In addition, rat bilateral 14 gauge punches were collected from substantia nigra and red nucleus (as anatomical controls), and VTA, and processed for Western blotting as described below (Supplementary Fig. 4).

Stereotaxic surgery—Mice or rats were anesthetized with ketamine (100 mg/kg) and xylazine (10 mg/kg). 33 gauge needles were used to bilaterally infuse HSVs or LVs into VTA [for mice, AP = −3.2, ML = ±1.0, DV = −4.6; for rats, AP = −5.5, ML = ±2.0, DV = −7.4 from Bregma (mm), 7° angle]. An infusion volume of 0.5 μl (mice) or 1.0 μl (rats) was delivered using 5 μl Hamilton syringe over the course of 5 min [at a rate of 0.1 μl/min (mice) or 0.2 μl/min (rats)]. The infusion needle remained in place for at least 5 min after the infusions before removal to prevent backflow of the injected material.

RNA isolation and qPCR—Total RNA was isolated from postmortem human brain specimens using Arcturus Pico Pure kit (Life Technologies) and from frozen VTA bilateral punches (rat, 14-gauge; mouse, 15-gauge) using Trizol (Life Technologies) and a micro RNeasy kit (Qiagen) as described[11]. RNA was reverse transcribed into cDNA using an iScript cDNA synthesis kit (BioRad). Primers were designed to amplify regions of 100–200 bp located within the genes of interest or chosen from previous studies[16,46]. All reactions were run in triplicate and analyzed using the ΔΔCt method[47] with glyceraldehyde-3-phosphate dehydrogenase (*Gapdh*) or 18S ribosomal RNA (*Rn18S*) as a normalization control. qPCR primers are listed in Supplementary Table 2.

Quantitative chromatin immunoprecipitation (qChIP)—Freshly dissected rat VTA punches were cross-linked with 1% formaldehyde, quenched with 2 M glycine, and sonicated to ~500 bp at 4°C. For each ChIP for histone modifications, bilateral 14-gauge VTA punches were used; for each ChIP for transcription factors, bilateral 14-gauge punches were pooled from two rats. Separate groups of animals were used for each qChIP experiment. Sheep anti-rabbit or anti-mouse IgG magnetic beads (Invitrogen) were prepared by incubating with antibodies of interest. Chromatin samples were immunoprecipitated with the conjugated bead/antibody mixtures, and then reverse cross-linked. DNA was purified and quantified using qPCR in triplicate from independent groups of animals. Normal mouse or rabbit IgG immunoprecipitations were performed as controls. Primers for most qChIPs, shown in Supplementary Table 3, were designed to amplify 150–200 bp products that include CREB binding sites. All ChIP antibodies were validated using qChIP (Supplementary Fig. 9) with rat primer sets that were designed, based on previous studies validating ChIP antibodies in other systems or on validation information provided by the manufacturers (Supplementary Table 4). The primer pairs for NURR1 CHIP validation (e.g.,

Bdnf, *Pitx3*, and *Th* primers) were designed to amplify 150–200 bp products that contain a NBRE (NGFI-B response element)–like sequence, which are putative NURR1 binding sites[30]. To further demonstrate the selectivity of anti-NURR1, we performed Western blotting using anti-NOR1 (rabbit polyclonal, Santa Cruz, sc-30154), anti-NUR77 (rabbit polyclonal, Santa Cruz, sc-5569), or anti-NURR1 (rabbit polyclonal, Santa Cruz, sc-991) on samples that were immunoprecipitated with anti-NURR1 (Supplementary Fig. 7c–e).

Immunohistochemistry—Immunohistochemistry was conducted according to published procedures[11]. For GFP/TH and TMT/TH double-labeling, brain sections were incubated in 1:4000 of anti-TH (T1299, Sigma) 1:2000 of rabbit polyclonal anti-GFP (A11122, Invitrogen), or 1:1000 of rabbit anti-dsRed (632496, Clontech), respectively, in block solution overnight at 4°C. The next day, sections were incubated in 1:500 of donkey anti-rabbit Cy2 (Immuno Research) for anti-GFP together with 1:500 of donkey anti-mouse Cy3 for anti-TH or 1:500 of donkey anti-rabbit Cy3 for anti-dsRed together with 1:500 of donkey anti-mouse Cy2 for anti-TH in PBS for 1 hr. For GFP/Cre double-labeling, 1:2000 of rabbit polyclonal anti-GFP (A11122, Invitrogen), 1:1000 mouse anti-Cre recombinase (MAB3120), 1:500 of donkey anti-rabbit Cy2, and 1:500 of donkey anti-mouse Cy3 were used. All sections were imaged on a LSM 710 confocal microscope (Zeiss) at 10× or 20× magnification. All histological procedures were replicated independently at least 2 times.

Western blotting—Western blotting analyses were conducted according to published procedures[15]. For primary antibody incubation, anti-EZH2 (1:1000; rabbit monoclonal, Cell Signaling, 5246S), anti-total-CREB (1:1000; rabbit monoclonal, Millipore, 17-600), and anti-NURR1 were used. Blots were imaged with the Odyssey Infrared Imaging system (Li-Cor) and quantified by densitometry using NIH ImageJ. The amount of protein blotted onto each lane was normalized to levels of tubulin. Western blot analyses were replicated at least twice.

Specific experiments

Experiment 1: *Bdnf* down-regulation by opiates—We examined the effect of opiate exposure on *Bdnf* mRNA expression in human, rat, and mosue VTA. Total RNA was isolated from postmortem brain specimens of human heroin addicts (n = 9) and controls (n = 5) (Supplementary Table 1). VTA punches (bilateral, 14-gauge) were collected from previously frozen brains of rats that were killed 24 hr after the final heroin self-administration session (n = 24) (Supplementary Fig. 1b). We also freshly dissected 14-gauge bilateral rat VTA punches 30 min after completing the last locomotor activity test on day 28 (Supplementary Fig. 1c), after 14 days withdrawal from 14 days of prior morphine administration (n = 18). Mouse VTA punches (bilateral, 15-gauge) were freshly dissected 1 hr after completing morphine CPP test sessions (n = 24) (Supplementary Fig. 1d).

Experiment 2: Stalling of Pol II at *Bdnf* promoters by morphine—For each ChIP sample, VTA punches were pooled from two rats (4 punches) that were killed on day 28, after 14 days withdrawal from 14 days of prior morphine administration (n = 20 or 24). Anti-total-Pol II (mouse monoclonal, Millipore, 05-623), anti-phospho-Ser2-Pol II (antibody to Pol II phosphorylated at Ser2 of its C terminal domain) (mouse monoclonal, Abcam,

ab24758), or anti-phospho-Ser5-Pol II (rabbit polyclonal, Abcam, ab5131) were used for this experiment. Primers for qChIP with anti-total-Pol II and anti-phospho-Ser5-Pol II were designed to amplify 150–200 bp products that include CREB binding sites of *Bdnf* promoters. Primers for qChIP with anti-phospho-Ser2-Pol II were designed to amplify 150–200 bp products within the coding sequence of the *Bdnf* gene (Supplementary Table 3).

Experiment 3: Histone modifications by morphine—For each ChIP sample for histone modifications, VTA punches (2 punches) were collected from one control or chronic morphine-treated rat (14 days of morphine administration followed by 14 days of withdrawal) (n = 8 -11 for each ChIP). For each ChIP sample for key histone modifying enzymes and related regulatory proteins, VTA punches were pooled from two rats (4 punches) (n = 14 – 22). Anti-acH3 (rabbit polyclonal, Millipore, 06-599), anti-acH4 (rabbit polyclonal, Millipore, 06-598), anti-H3K4me3 (rabbit monoclonal, Millipore, 17-614), anti-H3K9me2 (mouse monoclonal, Abcam, ab1220), anti-H3K9me3 (rabbit polyclonal, Abcam, ab8898), anti-H3K27me3 (mouse monoclonal, Abcam, ab6002), anti-H3K36me3 (rabbit polyclonal, Abcam, ab9050), anti-mSIN3a (rabbit polyclonal, Santa Cruz, sc-994X), anti-ING2 (rabbit polyclonal, Santa Cruz, sc-134973), anti-KMT2A/MLL (rabbit polyclonal, Millipore, ABE240), anti-KMT1C/G9a (rabbit polyclonal, Abcam, ab40542), anti-SUZ12 (rabbit monoclonal, Cell Signaling, 3737S), anti-EZH2, anti-RING1A (rabbit polyclonal, Abcam, ab32644), anti-RING1B (rabbit monoclonal, Cell Signaling, 5694S), and anti-BMI1 (rabbit monoclonal, Cell Signaling, 6964S) were used.

Experiment 4: Role of EZH2 in *Bdnf* expression and morphine CPP—Stereotaxic surgery was performed on adult male c57BL/6 mice (8 weeks) to inject HSV-EZH2-GFP or HSV-GFP into the VTA. The first batch of mice (n = 18) was killed for qPCR for validation (Supplementary Fig. 3a) and *Bdnf* expression (Fig. 3h) 4 days after stereotaxic surgery. Viral injection sites were confirmed using standard histological methods (see Fig. 3g) using VTA sections from a subset of HSV-EZH2 infused mice (n = 3). A second batch of mice (n = 24) was used for morphine CPP (Fig. 3i). Two days after the surgery, mice were conditioned in a three-chambered CPP box for three days. The next day, animals were given a final CPP test.

Separate groups of rats were bilaterally injected with LV-shRNA-EZH2 (iV000225, Applied Biological Materials, Canada) or LV-shRNA-scramble (LVP015-G) in VTA. The first batch of rats (n = 22) was killed for qPCR for validation (Supplementary Fig. 3c) 10 days after stereotaxic surgery. Viral injection sites were confirmed using standard histological methods (Supplementary Fig. 3b) using VTA sections from a subset of LV-shRNA-EZH2 infused rats (n = 3). A second batch of rats (n = 14) was used for qPCR for *Bdnf* expression after chronic morphine treatment (Supplementary Fig. 3d). Briefly, we first injected morphine (5 mg/kg, IP) for 14 days and bilateral viral injections with LVs were performed 4 days after the last morphine injection. Rats were killed and VTA punches (bilateral, 14-gauge) were collected 10 days after surgery.

Experiment 5: Role of CREB in *Bdnf* expression—For total- and phospho-CREB ChIP experiments, VTA punches were pooled from two chronic morphine-treated rats (14 days of morphine administration followed by 14 days of withdrawal) (n = 16 or 20 for each).

Anti-total-CREB and anti-phospho-CREB (rabbit polyclonal, Millipore, 06-519) were used for immunoprecipitation. In separate groups of animals, we performed stereotaxic surgery on male c57BL/6 mice or floxed CREB mice to inject HSV-CREB or HSV-Cre and their controls (HSV-TMT or HSV-GFP, respectively) into the VTA. The HSV-CREB/HSV-TMT infused c57BL/6 mice (n = 17) and HSV-Cre/HSV-GFP infused floxed CREB mice (n = 20) were killed for qPCR for validation (Supplementary Fig. 5a,b) and *Bdnf* expression (Fig. 4d,f) 4 days after stereotaxic surgery. Viral injection sites were confirmed using standard histological methods (Fig. 4c,e) using VTA sections from a subset of HSV-CREB or HSV-Cre infused mice (n = 3 each).

Experiment 6: Epigenetic mechanism of *Bdnf* regulation: interaction between pCREB and H3K27me3—Stereotaxic surgery was performed on adult rats to inject HSV-EZH2 or HSV-GFP into the VTA. Two batches of rats were killed for H3K27me3 ChIP (n = 14) and pCREB ChIP (n = 22) at *Bdnf* promoters (Fig. 4g,h) 4 days after stereotaxic surgery. For these ChIP experiments, VTA punches were pooled from two rats. For H3K27me3 ChIP experiment, punches from one rat were used. mRNA levels of *Bdnf* exon IX were also measured using cDNA derived from VTA of HSV-EZH2 or -GFP infused mice (from **Experiment 4**) (Supplementary Fig. 3a). ChIP experiments with anti-phospho-CREB, anti-total-CREB, and anti-H3K27me3 were also conducted at *Bdnf* promoter regions with VTA punches from heroin self-administered rats (anti-phospho-CREB, n = 20; anti-total-CREB, n = 14; anti-H3K27me3, n = 11) (Supplementary Fig. 6d–f).

Another set of ChIP experiments with anti-phospho-CREB, anti-total-CREB, and anti-H3K27me3 was conducted as a control at *Th* and *Gria1* promoter regions with control and chronic morphine-treated rats (14 days of morphine administration followed by 14 days of withdrawal) (anti-phospho-CREB, n = 32; anti-total-CREB, n = 18; anti-H3K27me3, n = 10) (Supplementary Fig. 6a–c).

Experiment 7: Epigenetic mechanism of *Bdnf* regulation: interaction between NURR1 and CREB—ChIP experiment with anti-NURR1 was conducted at *Bdnf* promoters with chronic morphine-treated rats (14 days of morphine administration followed by 14 days of withdrawal) (n = 18). Another set of ChIP experiments with anti-H3K27me3 and anti-phospho-CREB was conducted at *Nurr1* promoter regions with chronic morphine-treated rats (anti-H3K27me3, n = 10; anti-phospho-CREB, n = 36). In separate experiments, stereotaxic surgery was performed on rats to inject HSV-CREB or HSV-TMT into the VTA. Two batches of rats were killed for total- (n = 20) and phospho- (n = 20) CREB ChIP at the *Nurr1* promoter (Supplementary Fig. 5c,d). For NURR1 ChIP and total-/phospho-CREB ChIP experiments, VTA punches were pooled from two rats. For H3K27me3 ChIP experiment, bilateral punches from one rat were used. *Nurr1* mRNA levels in VTA were also measured using cDNA derived from chronic morphine-treated rats, from heroin self-administering rats, or from HSV-CREB infused mice generated from prior experiments.

Experiment 8: Behavioral and molecular effects of NURR1—We performed stereotaxic surgery on rats to inject HSV-NURR1 or HSV-TMT into the VTA. The rats (n = 19) were killed for qPCR validation (Supplementary Fig. 7a) and *Bdnf* expression (Fig. 5j) 4

days after stereotaxic surgery. Viral injection sites were confirmed using standard histological methods (Fig. 5i) using VTA sections from a subset of HSV-NURR1 infused rats (n = 3). Another set of rats was given daily injection of morphine (5 mg/kg, IP; n = 27) or saline (n = 11) for 14 days. Each morphine-/saline-injected batch was then re-exposed to morphine (5 mg/kg, IP) or saline on day 28. All of these rats underwent locomotor activity tests on day 0, 14, and 28 and stereotaxic surgery with HSV-NURR1 or HSV-TMT into the VTA 10 days after the last injection of chronic morphine or saline (on day 24) (Fig. 5g,h and Supplementary Fig. 7b). In a separate experiment, stereotaxic surgery was performed on adult male c57BL/6 mice (8 weeks) or floxed BDNF mice to inject HSV-NURR1, HSV-TMT, and/or HSV-Cre into the VTA. In case of floxed BDNF mice, we infused 0.25 μl of HSV-NURR1 or HSV-TMT together with 0.25 μl of HSV-Cre. Two days after the surgery, the HSV-NURR1/HSV-TMT infused c57BL/6 mice (n = 15) and HSV-NURR+HSV-Cre/HSV-TMT+HSV-Cre infused floxed BDNF mice (n = 19) were conditioned in a three-chambered CPP box for three days. The next day, animals were given a final CPP test.

Statistical analysis

Sample sizes were similar to those reported in previous works and based on expected effect sizes and power analyses[1,7,11,15,28,42,44,48]. Data were collected and processed randomly and analyzed with SigmaPlot 12.5 (Systat) and Prism 5.0 (GraphPad). Data collection and analysis were not performed blind to the conditions of the experiments. Normality (Shapiro-Wilk test) and equal variance (F-test) assumptions were confirmed before parametric analysis, unless otherwise indicated. For normally distributed data, Student's t-tests were used to assess differences between two experimental groups. For a two-sample comparison of means with unequal variances, Student's t-tests with Welch's correction were used. One-way ANOVAs were used for analysis of three or more groups, followed by Fisher's PLSD *post hoc* tests. For all qChIP analyses, two-way ANOVAs with Fisher's PLSD *post hoc* tests were used. For locomotor activity and heroin self-administration data, a repeated-measures two-way ANOVA was used followed by Fisher's PLSD *post hoc* tests. Main and interaction effects were considered significant at $p < 0.05$. Mann-Whitney U tests were performed to compare two columns of non-normally distributed data. Outliers were excluded from analysis when identified by Grubbs' test. Bar graphs show mean ± SEM. Box plots present, in ascending order, minimum sample value, first quartile, median, third quartile, maximum sample value. Individual statistical values are available in the Supplementary Methods Checklist.

Supplementary Material

Refer to Web version on PubMed Central for supplementary material.

Acknowledgments

We thank Ted Abel (University of Pennsylvania) for helpful discussions. This work was supported by grants from the National Institute on Drug Abuse (E.J.N., M.M.-R.).

References

1. Lobo MK, et al. Cell type-specific loss of BDNF signaling mimics optogenetic control of cocaine reward. Science. 2010; 330:385–390. [PubMed: 20947769]
2. Pu L, Liu QS, Poo MM. BDNF-dependent synaptic sensitization in midbrain dopamine neurons after cocaine withdrawal. Nat Neurosci. 2006; 9:605–607. [PubMed: 16633344]
3. Russo SJ, Mazei-Robison MS, Ables JL, Nestler EJ. Neurotrophic factors and structural plasticity in addiction. Neuropharmacology. 2009; 56 (Suppl 1):73–82. [PubMed: 18647613]
4. Filip M, et al. Alterations in BDNF and trkB mRNAs following acute or sensitizing cocaine treatments and withdrawal. Brain Res. 2006; 1071:218–225. [PubMed: 16423334]
5. Graham DL, et al. Dynamic BDNF activity in nucleus accumbens with cocaine use increases self-administration and relapse. Nat Neurosci. 2007; 10:1029–1037. [PubMed: 17618281]
6. Grimm JW, et al. Time-dependent increases in brain-derived neurotrophic factor protein levels within the mesolimbic dopamine system after withdrawal from cocaine: implications for incubation of cocaine craving. J Neurosci. 2003; 23:742–747. [PubMed: 12574402]
7. Graham DL, et al. Tropomyosin-related kinase B in the mesolimbic dopamine system: region-specific effects on cocaine reward. Biol Psychiatry. 2009; 65:696–701. [PubMed: 18990365]
8. Hall FS, Drgonova J, Goeb M, Uhl GR. Reduced behavioral effects of cocaine in heterozygous brain-derived neurotrophic factor (BDNF) knockout mice. Neuropsychopharmacology. 2003; 28:1485–1490. [PubMed: 12784114]
9. Horger BA, et al. Enhancement of locomotor activity and conditioned reward to cocaine by brain-derived neurotrophic factor. J Neurosci. 1999; 19:4110–4122. [PubMed: 10234039]
10. Lu L, Dempsey J, Liu SY, Bossert JM, Shaham Y. A single infusion of brain-derived neurotrophic factor into the ventral tegmental area induces long-lasting potentiation of cocaine seeking after withdrawal. J Neurosci. 2004; 24:1604–1611. [PubMed: 14973246]
11. Koo JW, et al. BDNF is a negative modulator of morphine action. Science. 2012; 338:124–128. [PubMed: 23042896]
12. Berhow MT, et al. Influence of neurotrophic factors on morphine- and cocaine-induced biochemical changes in the mesolimbic dopamine system. Neuroscience. 1995; 68:969–979. [PubMed: 8545003]
13. Russo SJ, et al. IRS2-Akt pathway in midbrain dopamine neurons regulates behavioral and cellular responses to opiates. Nat Neurosci. 2007; 10:93–99. [PubMed: 17143271]
14. Sklair-Tavron L, et al. Chronic morphine induces visible changes in the morphology of mesolimbic dopamine neurons. Proc Natl Acad Sci U S A. 1996; 93:11202–11207. [PubMed: 8855333]
15. Mazei-Robison MS, et al. Role for mTOR signaling and neuronal activity in morphine-induced adaptations in ventral tegmental area dopamine neurons. Neuron. 2011; 72:977–990. [PubMed: 22196333]
16. Aid T, Kazantseva A, Piirsoo M, Palm K, Timmusk T. Mouse and rat BDNF gene structure and expression revisited. J Neurosci Res. 2007; 85:525–535. [PubMed: 17149751]
17. Vanderschuren LJ, et al. Morphine-induced long-term sensitization to the locomotor effects of morphine and amphetamine depends on the temporal pattern of the pretreatment regimen. Psychopharmacology (Berl). 1997; 131:115–122. [PubMed: 9201798]
18. Komarnitsky P, Cho EJ, Buratowski S. Different phosphorylated forms of RNA polymerase II and associated mRNA processing factors during transcription. Genes Dev. 2000; 14:2452–2460. [PubMed: 11018013]
19. Laherty CD, et al. Histone deacetylases associated with the mSin3 corepressor mediate mad transcriptional repression. Cell. 1997; 89:349–356. [PubMed: 9150134]
20. Shi X, et al. ING2 PHD domain links histone H3 lysine 4 methylation to active gene repression. Nature. 2006; 442:96–99. [PubMed: 16728974]
21. Ythier D, et al. Sumoylation of ING2 regulates the transcription mediated by Sin3A. Oncogene. 2010; 29:5946–5956. [PubMed: 20676127]

22. Czermin B, et al. Drosophila enhancer of Zeste/ESC complexes have a histone H3 methyltransferase activity that marks chromosomal Polycomb sites. Cell. 2002; 111:185–196. [PubMed: 12408863]
23. Muller J, et al. Histone methyltransferase activity of a Drosophila Polycomb group repressor complex. Cell. 2002; 111:197–208. [PubMed: 12408864]
24. Simon JA, Kingston RE. Mechanisms of polycomb gene silencing: knowns and unknowns. Nat Rev Mol Cell Biol. 2009; 10:697–708. [PubMed: 19738629]
25. Cao R, Tsukada Y, Zhang Y. Role of Bmi-1 and Ring1A in H2A ubiquitylation and Hox gene silencing. Mol Cell. 2005; 20:845–854. [PubMed: 16359901]
26. Tao X, West AE, Chen WG, Corfas G, Greenberg ME. A calcium-responsive transcription factor, CaRF, that regulates neuronal activity-dependent expression of BDNF. Neuron. 2002; 33:383–395. [PubMed: 11832226]
27. Walters CL, Kuo YC, Blendy JA. Differential distribution of CREB in the mesolimbic dopamine reward pathway. J Neurochem. 2003; 87:1237–1244. [PubMed: 14622103]
28. Olson VG, et al. Regulation of drug reward by cAMP response element-binding protein: evidence for two functionally distinct subregions of the ventral tegmental area. J Neurosci. 2005; 25:5553–5562. [PubMed: 15944383]
29. Xiong Y, et al. Polycomb antagonizes p300/CREB-binding protein-associated factor to silence FOXP3 in a Kruppel-like factor-dependent manner. J Biol Chem. 2012; 287:34372–34385. [PubMed: 22896699]
30. Volpicelli F, et al. Direct regulation of Pitx3 expression by Nurr1 in culture and in developing mouse midbrain. PLoS One. 2012; 7:e30661. [PubMed: 22363463]
31. Volpicelli F, et al. Bdnf gene is a downstream target of Nurr1 transcription factor in rat midbrain neurons in vitro. J Neurochem. 2007; 102:441–453. [PubMed: 17506860]
32. Barneda-Zahonero B, et al. Nurr1 protein is required for N-methyl-D-aspartic acid (NMDA) receptor-mediated neuronal survival. J Biol Chem. 2012; 287:11351–11362. [PubMed: 22294685]
33. Kadkhodaei B, et al. Nurr1 is required for maintenance of maturing and adult midbrain dopamine neurons. J Neurosci. 2009; 29:15923–15932. [PubMed: 20016108]
34. McEvoy AN, et al. Activation of nuclear orphan receptor NURR1 transcription by NF-kappa B and cyclic adenosine 5′-monophosphate response element-binding protein in rheumatoid arthritis synovial tissue. J Immunol. 2002; 168:2979–2987. [PubMed: 11884470]
35. Chu NN, et al. Peripheral electrical stimulation reversed the cell size reduction and increased BDNF level in the ventral tegmental area in chronic morphine-treated rats. Brain Res. 2007; 1182:90–98. [PubMed: 17945205]
36. Vargas-Perez H, et al. Ventral tegmental area BDNF induces an opiate-dependent-like reward state in naive rats. Science. 2009; 324:1732–1734. [PubMed: 19478142]
37. Fujii S, Ito K, Ito Y, Ochiai A. Enhancer of zeste homologue 2 (EZH2) down-regulates RUNX3 by increasing histone H3 methylation. J Biol Chem. 2008; 283:17324–17332. [PubMed: 18430739]
38. van der Vlag J, Otte AP. Transcriptional repression mediated by the human polycomb-group protein EED involves histone deacetylation. Nat Genet. 1999; 23:474–478. [PubMed: 10581039]
39. Milne TA, et al. MLL targets SET domain methyltransferase activity to Hox gene promoters. Mol Cell. 2002; 10:1107–1117. [PubMed: 12453418]
40. Xia ZB, Anderson M, Diaz MO, Zeleznik-Le NJ. MLL repression domain interacts with histone deacetylases, the polycomb group proteins HPC2 and BMI-1, and the corepressor C-terminal-binding protein. Proc Natl Acad Sci U S A. 2003; 100:8342–8347. [PubMed: 12829790]
41. Rios M, et al. Conditional deletion of brain-derived neurotrophic factor in the postnatal brain leads to obesity and hyperactivity. Mol Endocrinol. 2001; 15:1748–1757. [PubMed: 11579207]
42. Covington HE 3rd, et al. A role for repressive histone methylation in cocaine-induced vulnerability to stress. Neuron. 2011; 71:656–670. [PubMed: 21867882]
43. Anderson SA, et al. Impaired periamygdaloid-cortex prodynorphin is characteristic of opiate addiction and depression. J Clin Invest. 2013; 123:5334–5341. [PubMed: 24231353]

44. Barrot M, et al. CREB activity in the nucleus accumbens shell controls gating of behavioral responses to emotional stimuli. Proc Natl Acad Sci U S A. 2002; 99:11435–11440. [PubMed: 12165570]
45. Dietz DM, et al. Rac1 is essential in cocaine-induced structural plasticity of nucleus accumbens neurons. Nat Neurosci. 2012; 15:891–896. [PubMed: 22522400]
46. Liu QR, et al. Rodent BDNF genes, novel promoters, novel splice variants, and regulation by cocaine. Brain Res. 2006; 1067:1–12. [PubMed: 16376315]
47. Livak KJ, Schmittgen TD. Analysis of relative gene expression data using real-time quantitative PCR and the 2(-Delta Delta C(T)) Method. Methods. 2001; 25:402–408. [PubMed: 11846609]
48. Schmidt HD, et al. Increased brain-derived neurotrophic factor (BDNF) expression in the ventral tegmental area during cocaine abstinence is associated with increased histone acetylation at BDNF exon I-containing promoters. J Neurochem. 2012; 120:202–209. [PubMed: 22043863]
49. Xu YX, Manley JL. Pin1 modulates RNA polymerase II activity during the transcription cycle. Genes Dev. 2007; 21:2950–2962. [PubMed: 18006688]
50. Sandoval J, et al. RNAPol-ChIP: a novel application of chromatin immunoprecipitation to the analysis of real-time gene transcription. Nucleic Acids Res. 2004; 32:e88. [PubMed: 15247321]
51. Egloff S, Al-Rawaf H, O'Reilly D, Murphy S. Chromatin structure is implicated in "late" elongation checkpoints on the U2 snRNA and beta-actin genes. Mol Cell Biol. 2009; 29:4002–4013. [PubMed: 19451231]
52. Khobta A, Anderhub S, Kitsera N, Epe B. Gene silencing induced by oxidative DNA base damage: association with local decrease of histone H4 acetylation in the promoter region. Nucleic Acids Res. 2010; 38:4285–4295. [PubMed: 20338881]
53. Weishaupt H, Attema JL. A Method to Study the Epigenetic Chromatin States of Rare Hematopoietic Stem and Progenitor Cells; MiniChIP-Chip. Biol Proced Online. 2010; 12:1–17. [PubMed: 21406121]
54. Nitzsche A, Steinhausser C, Mucke K, Paulus C, Nevels M. Histone H3 lysine 4 methylation marks postreplicative human cytomegalovirus chromatin. J Virol. 2012; 86:9817–9827. [PubMed: 22761369]
55. Gilfillan GD, et al. Limitations and possibilities of low cell number ChIP-seq. BMC Genomics. 2012; 13:645. [PubMed: 23171294]
56. Marchesi I, Fiorentino FP, Rizzolio F, Giordano A, Bagella L. The ablation of EZH2 uncovers its crucial role in rhabdomyosarcoma formation. Cell Cycle. 2012; 11:3828–3836. [PubMed: 22983009]
57. Lee TI, et al. Control of developmental regulators by Polycomb in human embryonic stem cells. Cell. 2006; 125:301–313. [PubMed: 16630818]
58. Schaefer A, et al. Control of cognition and adaptive behavior by the GLP/G9a epigenetic suppressor complex. Neuron. 2009; 64:678–691. [PubMed: 20005824]
59. Ren G, et al. Polycomb protein EZH2 regulates tumor invasion via the transcriptional repression of the metastasis suppressor RKIP in breast and prostate cancer. Cancer Res. 2012; 72:3091–3104. [PubMed: 22505648]
60. Rotman N, Guex N, Gouranton E, Wahli W. PPARbeta interprets a chromatin signature of pluripotency to promote embryonic differentiation at gastrulation. PLoS One. 2013; 8:e83300. [PubMed: 24367589]
61. Basu A, Wilkinson FH, Colavita K, Fennelly C, Atchison ML. YY1 DNA binding and interaction with YAF2 is essential for Polycomb recruitment. Nucleic Acids Res. 2014; 42:2208–2223. [PubMed: 24285299]
62. Richly H, et al. Transcriptional activation of polycomb-repressed genes by ZRF1. Nature. 2010; 468:1124–1128. [PubMed: 21179169]
63. Mao L, et al. Cyclin E1 is a common target of BMI1 and MYCN and a prognostic marker for neuroblastoma progression. Oncogene. 2012; 31:3785–3795. [PubMed: 22120721]
64. Ellison-Zelski SJ, Solodin NM, Alarid ET. Repression of ESR1 through actions of estrogen receptor alpha and Sin3A at the proximal promoter. Mol Cell Biol. 2009; 29:4949–4958. [PubMed: 19620290]

65. Pellegrini M, et al. Expression profile of CREB knockdown in myeloid leukemia cells. BMC Cancer. 2008; 8:264. [PubMed: 18801183]

66. Sakurada K, Ohshima-Sakurada M, Palmer TD, Gage FH. Nurr1, an orphan nuclear receptor, is a transcriptional activator of endogenous tyrosine hydroxylase in neural progenitor cells derived from the adult brain. Development. 1999; 126:4017–4026. [PubMed: 10457011]

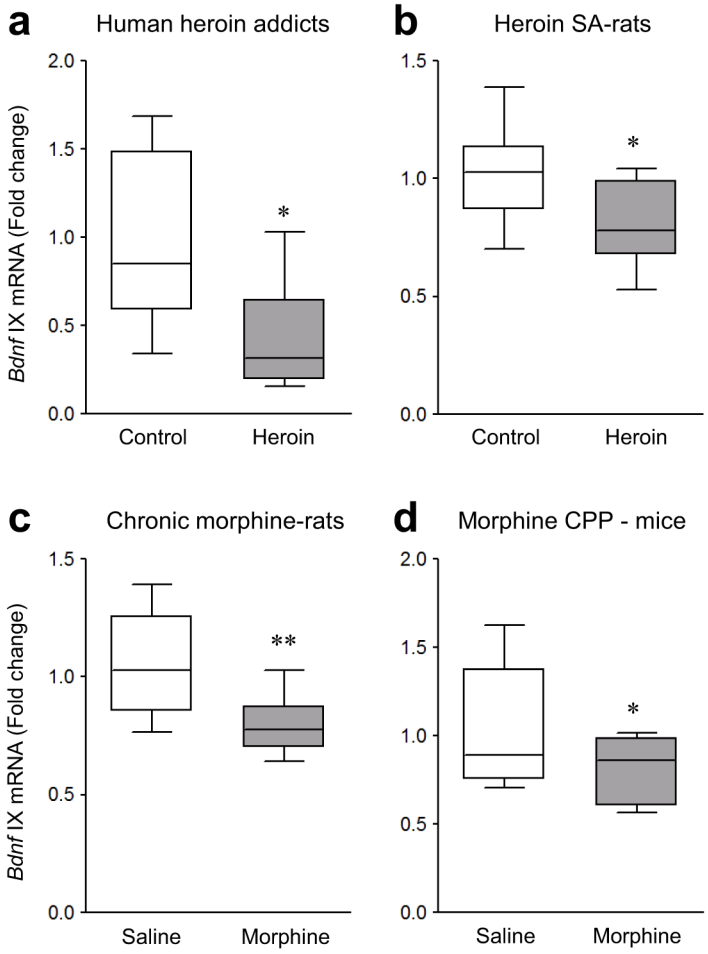

Figure 1.

Opiate-induced down-regulation of *Bdnf* expression in human, rat, and mouse VTA. (**a**) qPCR showed that mRNA levels of *Bdnf* exon IX were reduced in VTA of human heroin addicts compared to control subjects (unpaired Student's *t*-test, $t_{12} = 2.623$, $p = 0.0223$, $n =$ 5,9 human samples). (**b,c**) mRNA levels of *Bdnf* exon IX were decreased in VTA of heroin self-administering rats (**b**, *t*-test, $t_{22} = 2.793$, $p = 0.0106$, $n =$ 10,14 rats), and in VTA of rats given 14 daily morphine injections (5 mg/kg, IP) and examined after 14 days of withdrawal (**c**, *t*-test, $t_{16} = 2.923$, $p = 0.00995$, $n = 9$ rats), compared to respective control groups. (**d**) Morphine conditioned place preference (CPP) (15 mg/kg, IP) also decreased mRNA levels of *Bdnf* exon IX in mouse VTA compared to saline-treated mice (*t*-test, $t_{22} = 2.155$, $p =$ 0.0423, $n = 12$ mice). Unpaired *t*-tests, $^*p < 0.05$ and $^{**}p < 0.01$. Box plots present, in ascending order, minimum sample value, first quartile, median, third quartile, maximum sample value.

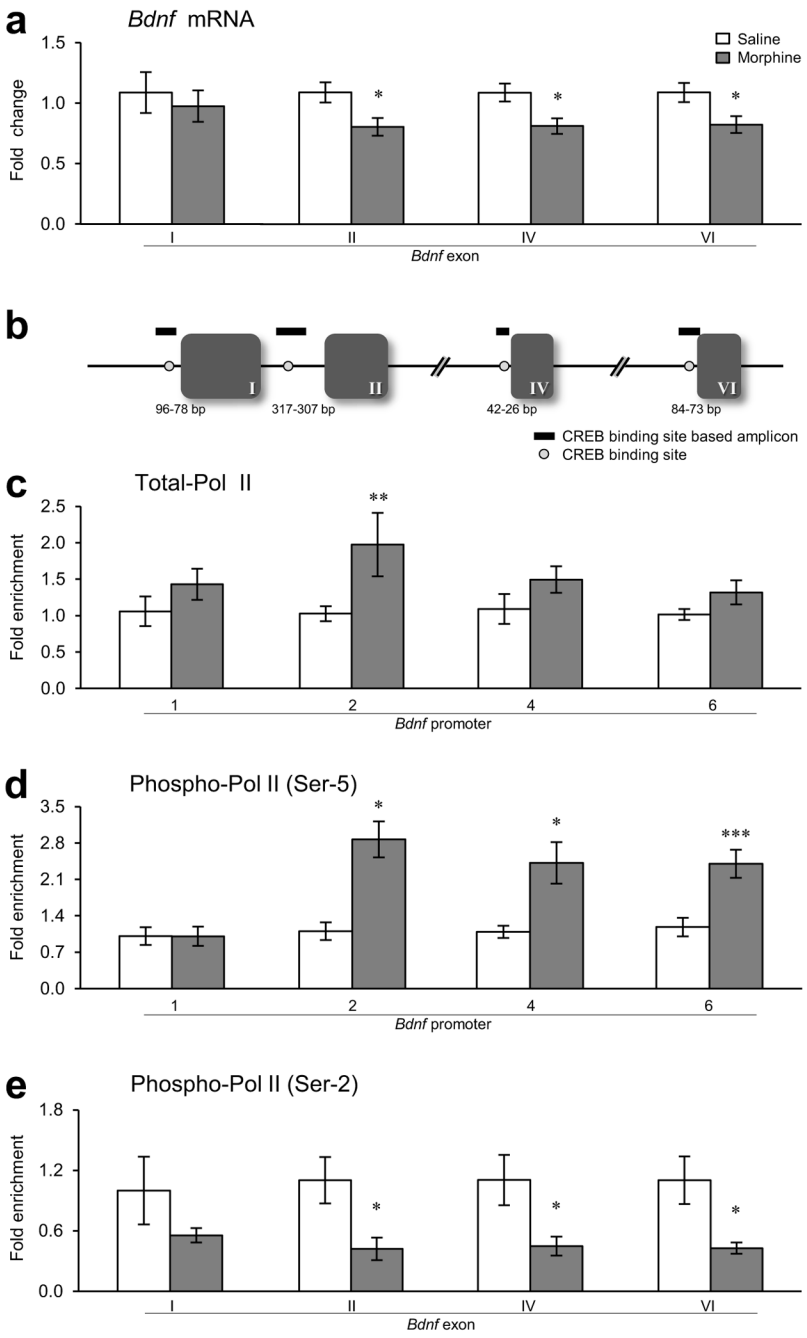

Figure 2.

Effect of chronic morphine on expression of *Bdnf* exons and on binding of Pol II to the *Bdnf* gene in rat VTA. (**a**) qPCR showed that mRNA levels of *Bdnf* exons II, IV, and VI were decreased in rat VTA after chronic (14 days) morphine administration followed by 14 days of withdrawal (as in Fig. 1c) relative to saline controls [two-way analysis of variance (ANOVA), drug effect: $F_{1,64} = 12.898$, $p < 0.001$; region effect: $F_{3,64} = 0.923$, $p = 0.435$; drug×region effect: $F_{3,64} = 0.328$, $p = 0.805$, $n = 9$ rats]. (**b**) Schematic diagram depicting the relative position of amplicons (green thick lines) generated by primers used to quantify

immunoprecipitated chromatin-DNA. Exons are represented as boxes and the introns as lines. Numbers of the exons are indicated in roman numerals. The positions of CREB binding sites (red circles) at *Bdnf* promoter regions are indicated relative to the transcription start site of exon I (96-84 bp/90-78 bp), exon II (317-307 bp), exon IV (42-33 bp/36-26 bp), and exon VI (84-73 bp). Primer information is provided in Supplementary Table 3. (**c**) qChIP showed that binding of total-Pol II to *Bdnf*-p2 was increased in response to chronic morphine (drug effect: $F_{1,39}$ =13.279, $p < 0.001$; region effect: $F_{3,39} = 1.019$, $p = 0.395$; drug×region effect: $F_{3,39} = 1.096$, $p = 0.362$, $n = 6$ rats). (**d**) Binding of phospho-Ser5-Pol II to *Bdnf*-p2, -p4, and -p6 was also increased in VTA of morphine-treated rats (drug effect: $F_{1,31} = 18.820$, $p < 0.001$; region effect: $F_{3,31}$ =6.474, $p = 0.002$; drug×region effect: $F_{3,31}$= 2.069, $p = 0.069$, $n = 5$ rats). (**e**) In contrast, binding of phospho-Ser2-Pol II to *Bdnf*-eII, -eIV, and -eVI was decreased after morphine exposure (drug effect: $F_{1,32} = 19.921$, $p < 0.001$; region effect: $F_{3,32} = 0.00309$, $p = 1.000$; drug×region effect: $F_{3,32} = 0.165$, $p = 0.919$, $n = 5$ rats). Two-way ANOVA with Fisher's protected least significant difference (PLSD) *post hoc* tests, *$p < 0.05$, **$p < 0.01$, and ***$p < 0.001$. Bar graphs show mean ± SEM.

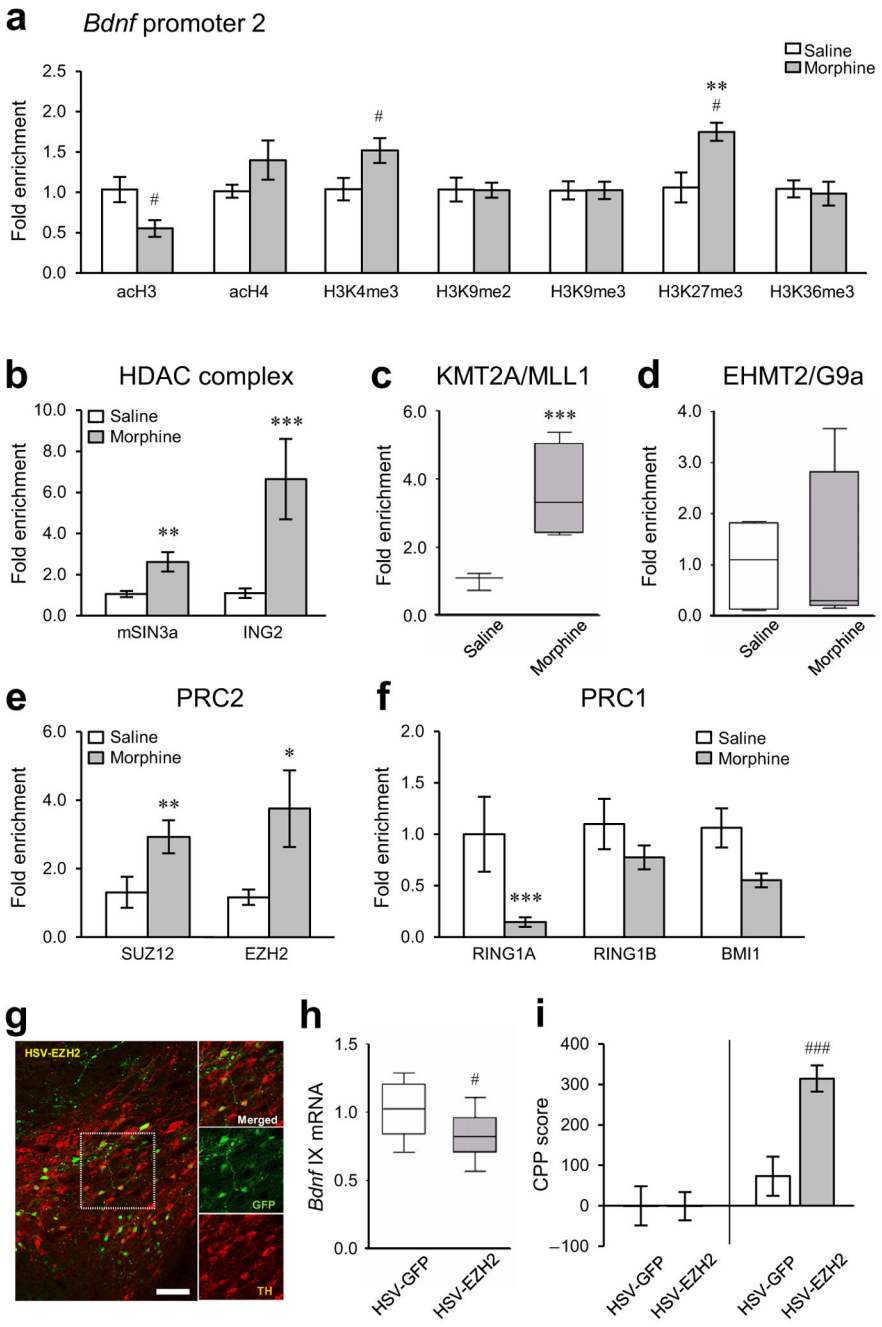

Figure 3.

Morphine-induced histone modifications at *Bdnf* promoters in rat VTA. (**a**) qChIP showed that chronic morphine (14 days of morphine administration followed by 14 days of withdrawal; Fig. 1c) selectively altered H3K27me3 (two-way ANOVA, drug effect: $F_{1,22}$ = 0.144, p = 0.708; region effect: $F_{3,22}$ = 6.442, p = 0.003; drug×region effect: $F_{3,22}$ = 6.178, p = 0.003, n = 4 rats, Supplementary Fig. 2f) at *Bdnf*-p2, particularly. Chronic morphine changed acH4 (drug effect: $F_{1,27}$ = 11.509, p = 0.002; region effect: $F_{3,27}$ = 0.482, p = 0.698; drug×region effect: $F_{3,27}$ = 0.184, p = 0.906, n = 5, 4 rats, Supplementary Fig. 2b) at

Bdnf-p4 in rat VTA, with no changes seen in several other histone modifications analyzed. Additional *post hoc* analyses with Student's *t*-tests showed that chronic morphine also changed acH3 (unpaired *t*-test, t_6= 2.581, p = 0.0417, n = 4 rats) and H3K4me3 (*t*-test, t_8 = 2.312, p = 0.0495, n = 5 rats) at *Bdnf*-p2 in VTA. Histone modifications by chronic morphine at other *Bdnf* promoters (*Bdnf*-p1, -p4, and -p6) are available in the Supplementary Fig. 2a–g. (**b**) Binding of mSIN3a (two-way ANOVA, drug effect: $F_{1,36}$ = 25.829, p < 0.001; region effect: $F_{3,36}$ = 0.541, p = 0.653; drug×region effect: $F_{3,36}$ = 0.464, p = 0.709, n = 6,5 rats) and ING2 (drug effect: $F_{1,28}$ = 37.786, p < 0.001; region effect: $F_{3,28}$ = 2.450, p = 0.614; drug×region effect: $F_{3,28}$ = 0.552, p = 0.651, n = 5,4 rats), core components of a major repressor complex, to *Bdnf*-p2 were increased by chronic morphine. (**c**) Consistent with enhancement in H3K4me3 levels, binding of MLL1 (KMT2A) to *Bdnf*-p2 was increased by chronic morphine (drug effect: $F_{1,23}$ = 24.884, p < 0.001; region effect: $F_{3,23}$ = 2.285, p = 0.106; drug×region effect: $F_{3,23}$ = 2.177, p = 0.118, n = 4 rats). (**d**) There was no morphine-induced alteration in binding of G9a (EHMT2) to *Bdnf*-p2 (drug effect: $F_{1,27}$ = 0.00384, p = 0.951; region effect: $F_{3,27}$ = 0.153, p = 0.927; drug×region effect: $F_{3,27}$ = 0.153, p = 0.927, n = 5,4 rats). (**e**) Consistent with enhancement in H3K27me3 levels, binding of SUZ12 (drug effect: $F_{1,24}$ = 12.662, p = 0.002; region effect: $F_{3,24}$ = 1.211, p = 0.327; drug×region effect: $F_{3,24}$ = 0.526, p = 0.668, n = 4 rats) and EZH2 (drug effect: $F_{1,20}$ =16.872, p < 0.001; region effect: $F_{3,20}$ = 1.209, p = 0.332; drug×region effect: $F_{3,20}$ = 1.111, p = 0.368, n = 4,3 rats), members of PRC2, to *Bdnf*-p2 was enhanced by chronic morphine. (**f**) In contrast, binding of PRC1 members, RING1A (drug effect: $F_{1,24}$ = 13.708, p < 0.001; region effect: $F_{3,24}$ = 0.0154, p = 0.997; drug×region effect: $F_{3,24}$ = 2.713, p = 0.067, n = 4 rats) and BMI1 (drug effect: $F_{1,32}$ = 10.975, p <= 0.002; region effect: $F_{3,32}$ = 0.117, p = 0.950; drug×region effect: $F_{3,32}$ = 0.0345, p = 0.991, n = 5 rats), to *Bdnf*-p2 were decreased by chronic morphine, but RING1B binding was unaffected (drug effect: $F_{1,23}$ =1.372, p = 0.253; region effect: $F_{3,23}$ = 0.267, p = 0.848; drug×region effect: $F_{3,23}$ = 0.298, p = 0.827, n = 4 rats). Morphine-induced epigenetic alterations by key histone modifying enzymes and related regulatory proteins at other *Bdnf* promoters (*Bdnf*- p1, -p4, and -p6) are available in Supplementary Fig. 2h–p. (**g**) Representative low-magnification photomicrographs with an inset depicting localized HSV-mediated EZH2 expression (GFP+, green) in dopaminergic neurons (TH+, red) in mouse VTA (scale bar, 50 μm). The results were replicated in three independent experiments. (**h**) Intra-VTA HSV-EZH2 suppressed the expression of *Bdnf* exon IX mRNA in mouse VTA compared to HSV-GFP controls (unpaired *t*-test, t_{16} = 2.168, p = 0.0456, n = 9 mice). (**i**) EZH2 overexpression in mouse VTA dramatically enhances morphine reward (*t*-test, t_{22} = 4.134, p = 0.000435, n = 12 mice). Two-way ANOVA with Fisher's PLSD *post hoc* tests, *p < 0.05, **p < 0.01, and ***p < 0.001; *t*-tests, $^{\#}p$ < 0.05 and $^{\#\#\#}p$ < 0.001. Bar graphs show mean ± SEM. Box plots present, in ascending order, minimum sample value, first quartile, median, third quartile, maximum sample value.

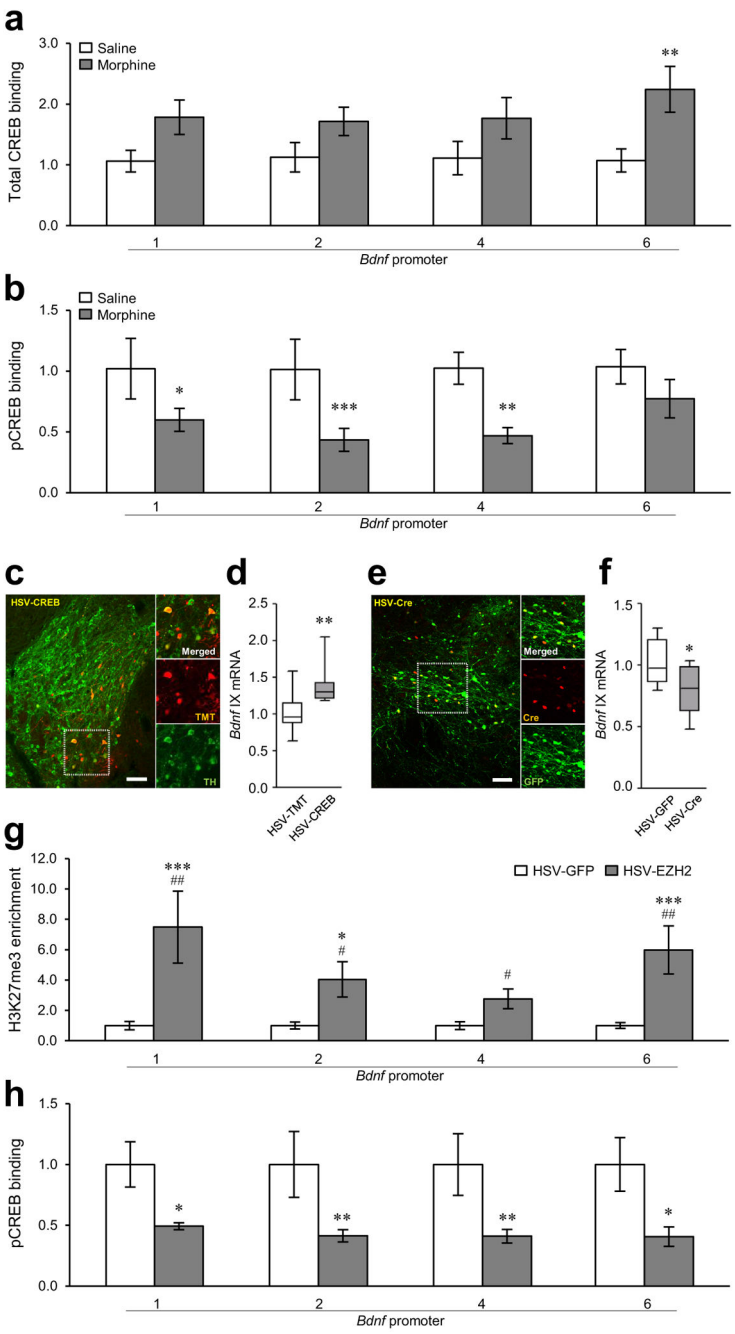

Figure 4.

Chronic morphine regulation of CREB binding to *Bdnf* promoters in VTA. (**a**) Chronic morphine (14 days of morphine administration followed by 14 days of withdrawal; Fig. 1c) increased total-CREB binding to *Bdnf*-p6 in rat VTA, with no effects seen at other *Bdnf* promoters (two-way ANOVA, drug effect: $F_{1,32} = 15.053$, $p < 0.001$; region effect: $F_{3,32} = 0.371$, $p = 0.774$; drug×region effect: $F_{3,32} = 0.412$, $p = 0.745$, $n = 5$ rats). (**b**) In contrast, chronic morphine reduced phospho-CREB binding to *Bdnf*-p1, -p2, and -p4 (drug effect: $F_{1,24} = 32.487$, $p < 0.001$; region effect: $F_{3,24} = 1.026$, $p = 0.399$; drug×region effect: $F_{3,24}$

= 0.834, p = 0.489, n = 4 rats). (**c**) Representative low-magnification photomicrographs with an inset depicting localized HSV-mediated CREB expression [tdTomato+ (TMT+), red] in dopaminergic neurons (TH+, green) in VTA of c57BL/6 mice (scale bar, 50 μm). (**d**) HSV-mediated CREB1 overexpression increases the expression of *Bdnf* exon IX in mouse VTA (Mann Whitney *U* test, U = 7, p = 0.006, n = 9,8 mice). (**e**) Representative low-magnification photomicrographs with an inset depicting localized HSV-mediated Cre expression (red) in dopaminergic neurons (TH+, green) in VTA of floxed CREB mice (scale bar, 50 μm). (**c,e**) Histological results were replicated in three independent experiments. (**f**) In contrast, knockdown of *Creb1* in the VTA of floxed CREB mice decreases the expression of *Bdnf* exon IX (unpaired *t*-test, t_{18} = 2.506, p = 0.0220, n = 10 mice). (**g**) HSV-mediated EZH2 overexpression (in the absence of morphine) significantly increased H3K27me3 levels at *Bdnf*-p1, -p2, and -p6 (two-way ANOVA, drug effect: $F_{1,48}$ = 35.413, p < 0.001; region effect: $F_{3,48}$ = 2.318, p = 0.087; drug×region effect: $F_{3,48}$ = 2.318, p = 0.087, n = 8,6 rats). Additional *post hoc* analyses with Mann Whitney *U* tests and Student's t-tests showed that EZH2 overexpression increased H3K27me3 levels at all *Bdnf*-promoters examined (*Bdnf*-p1, *U* test, U = 5, p = 0.013; *Bdnf*-p2, *t*-test, t_{12} = 2.957, p = 0.012; *Bdnf*-p4, *t*-test, t_{12} = 2.781, p = 0.0166; *Bdnf*-p6, *U* test, U =2, p = 0.003). (**h**) EZH2 overexpression significantly reduced phospho-CREB binding to *Bdnf*-p1, -p2, -p4, and -p6 (two-way ANOVA, drug effect: $F_{1,36}$ =25.091, p < 0.001; region effect: $F_{3,36}$ = 0.182, p = 0.908; drug×region effect: $F_{3,36}$ = 0.104, p = 0.957, n = 5,6 rats). (**a,b,g,h**) Two-way ANOVA with Fisher's PLSD *post hoc* tests, *p < 0.05, **p < 0.01, and ***p < 0.001; (**d**) Mann-Whitney *U* test, **p < 0.01; (**f**) Student's *t*-test, *p < 0.05; (**g**) Mann-Whitney *U* tests at *Bdnf*-p1 and -p6 and Student's *t*-tests at *Bdnf*-p2 and -p4, $^{\#}p$ < 0.05 and $^{\#\#}p$ < 0.01. Bar graphs show mean ± SEM. Box plots present, in ascending order, minimum sample value, first quartile, median, third quartile, maximum sample value.

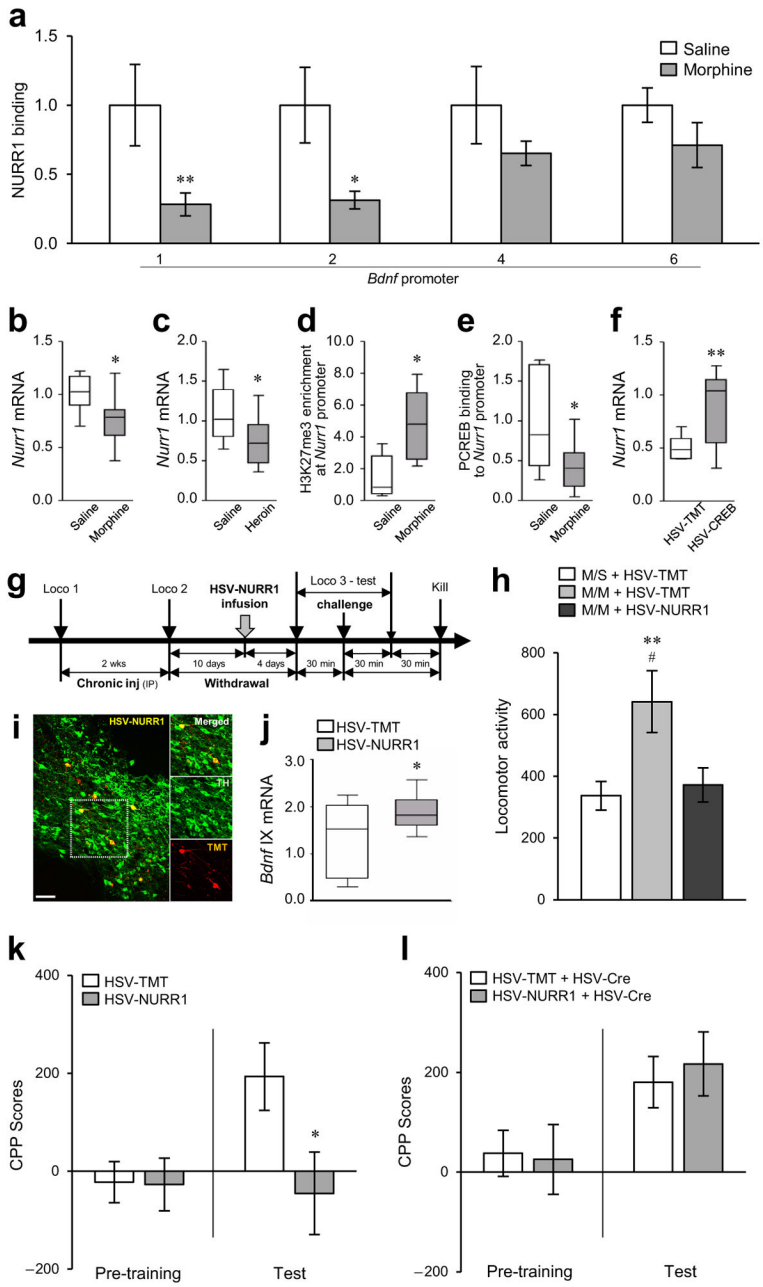

Figure 5.

Epigenetic regulation of *Bdnf* by NURR1 and its concomitant behavioral effects. (**a**) Chronic morphine (14 days of morphine administration followed by 14 days of withdrawal; Fig. 1c) decreased NURR1 binding to *Bdnf*-p1 and -p2 in rat VTA. Two-way ANOVA (drug effect: $F_{1,27} = 17.990$, $p < 0.001$; region effect: $F_{3,27} = 0.403$, $p = 0.752$; drug×region effect: $F_{3,27} = 0.990$, $p = 0.412$, $n = 4,5$ rats) with Fisher's PLSD *post hoc* tests, $^{*}p < 0.05$ and $^{**}p < 0.01$. (**b,c**) Chronic morphine (**b**, unpaired *t*-test, $t_{15} = 2.509$, $p = 0.0241$, $n = 9,8$ rats) and self-administered heroin (**c**, *t*-test, $t_{16} = 2.162$, $p = 0.0461$, $n = 8,10$ rats) decreased *Nurr1* mRNA expression in rat VTA. (**d**) H3K27me3 binding at the *Nurr1* gene promoter was

increased by chronic morphine in rat VTA (*t*-test, $t_8 = 2.733$, $p = 0.0257$, $n = 5$ rats). (**e**) Binding of phospho-CREB to the *Nurr1* gene promoter was decreased by chronic morphine in rat VTA (*t*-test, $t_{16} = 2.285$, $p = 0.0363$, $n = 10,8$ rats) (**f**) HSV-mediated CREB1 overexpression induced *Nurr1* expression in mouse VTA (unpaired *t*-test with Welch's correction, $t_{9.496} = 2.935$, $p = 0.0157$, $n = 9$ mice). (**g**) Scheme of the morphine treatment regimen used for locomotor tests in rats. HSV-NURR1 or its control HSV-TMT was infused into VTA of rats that were given chronic morphine (14 days, 5 mg/kg IP, followed by 10 days of withdrawal) and, 4 days later, the rats were challenged with morphine during the locomotor test. (**h**) Morphine-treated rats that were injected with HSV-TMT and then given a morphine challenge (M/M+HSV-TMT) showed higher locomotor activity compared to morphine-treated rats injected with HSV-TMT and then given a saline challenge (M/S +HSV-TMT). HSV-mediated overexpression of NURR1 in VTA blocked the morphine challenge-induced locomotor activation (M/M+HSV-NURR1). One-way ANOVA ($F_{2,24} = 4.712$, $p = 0.0188$, $n = 10,8,9$ rats) with Fisher's PLSD *post hoc* tests, $^{**}p < 0.01$ compared to M/S+HSV-TMT; $^{\#}p < 0.05$ compared to M/M+HSV-NURR1. (**i**) Representative low-magnification photomicrographs with an inset depicting localized HSV-NURR1 (TMT+, red) in dopaminergic neurons (TH+, green) of rat VTA (scale bar, 50 μm). The results were replicated in two independent experiments. (**j**) HSV-mediated NURR1 overexpression increased the expression of *Bdnf* exon IX mRNA in rat VTA (unpaired *t*-test with Welch's correction, $t_{10.98} = 2.440$, $p = 0.0328$, $n = 9,10$ rats). (**k**) NURR1 overexpression in mouse VTA significantly decreased morphine reward (15 mg/kg, IP) (unpaired *t*-test, $t_{13} = 2.165$, $p = 0.0496$, $n = 8,7$ mice). (**l**) However, there was no effect of NURR1 overexpression on morphine reward in mice with a local knockout of BDNF in VTA (*t*-test, $t_{17} = 0.4062$, $p = 0.690$, $n = 10,9$ mice). (**b–e,k,l**) Student's *t*-tests, $^{*}p < 0.05$; (**f,j**) Student's *t*-tests with Welch's correction, $^{*}p < 0.05$ and $^{**}p < 0.01$. Bar graphs show mean ± SEM. Box plots present, in ascending order, minimum sample value, first quartile, median, third quartile, maximum sample value.